Utilization of The Radiative Transfer Equation For High Precision Boundary Layer Modeling in Liquid Rocketry Applications

Phineas Masters[1], Rori Myers[2], Riley Powell[3], Zachary Moore[4], Vasilios Ekimogloy[5]

The University of Alabama in Huntsville, Huntsville, Alabama, 35805, USA

Abstract

Tartarus, the student liquid rocketry program of The Space Hardware Club of the University of Alabama in Huntsville, is currently working towards the completion of a demonstrator sub-scale rocket engine, Prometheus. To support modeling and safety analysis, the team has developed an in-house quasi-one-dimensional (Q1D) model to predict gas properties and firing behavior. To accurately characterize the effectiveness of fuel film cooling, it is necessary to take into account both convective and radiative heat transfer mechanisms. While convective heat transfer approximations are well studied and fairly precise, approximations of radiative heat transfer are typically significantly more simplistic and tend to introduce a significant amount of uncertainty into calculations of the heat flux into the film cooled length. Additionally, experimental results have proven that radiative heat transfer contributes a significant source of thermal loading to the film; robust models that produce higher fidelity results must be applied to develop a more complete model of the engine. This work presents a method of integrating the radiative heat transfer equation into a Q1D engine model to produce higher fidelity results without requiring the incredibly high level of computational power required to implement this equation into a computational fluid dynamic model. In doing so, this will produce a model not yet utilized or created at this level for the verification of cooling effectiveness.

I. Nomenclature

Variables

ε	=	emissivity
K_p	=	pressure correction factor
ρ	=	density $kg\ m^{-3}$
ρ_{opt}	=	optical density $atm\ m$
N	=	mole fraction
K_t	=	turbulence correction factor
p	=	pressure atm
P	=	pressure bar
A_w	=	wall absorptivity

[1] Undergraduate, Mechanical and Aerospace Engineering Dept, pgm0003@uah.edu, Student Member, 1604563.
[2] Undergraduate, Mechanical and Aerospace Engineering Dept, ndm0014@uah.edu, Student Member, 1811019.
[3] Undergraduate, Mechanical and Aerospace Engineering Dept, rmp0024@uah.edu, Student Member, 1923915.
[4] Undergraduate, Mechanical and Aerospace Engineering Dept, zdm0009@uah.edu, Student Member, 1422186.
[5] Undergraduate, Mechanical and Aerospace Engineering Dept, vekimogl@uah.edu, Student Member, 1823356.

D	=	diameter m
h	=	convective heat flux coefficient
G	=	mass velocity $kg\, m^{-2} s^{-1}$
c	=	specific heat $J\, kg^{-1} K^{-1}$
e_t	=	free stream turbulence intensity fraction
C_f	=	skin friction factor
Pr	=	Prandtl number
Re	=	Reynold’s number
x	=	distance from injection point
x_e	=	x corrected for developing pipe flow
μ	=	dynamic viscosity
u	=	axial velocity $m\, s^{-1}$
Γ_c	=	liquid coolant mass flow rate per circumference $kg\, s^{-1}\, m^{-1}$
$\dot{m}$	=	mass flow rate $kg\, s^{-1}$
t	=	film thickness m
τ	=	shear stress Pa
K_M	=	correction factor for molecular weight
M	=	molecular weight $g\, mol^{-1}$
$\dot{m}_v$	=	total liquid evaporation rate per surface area $kg\, m^{-2}\, s^{-1}$
σ	=	Stefan Boltzmann constant
$p_a L$	=	optical path length $bar\ cm$
P_E	=	equivalent pressure bar
h_{fg}	=	enthalpy of vaporization $J\, kg^{-1}$
h^*_{fg}	=	convective heat transfer coefficient from the hot gas to the coolant $J^2\, kg^{-2}$
q	=	heat flux $W\, m^{-2}$
F	=	blowing ratio
L_c	=	liquid film cooled length m
I	=	line intensity
n	=	normal vector m
s	=	length of ray cm
λ	=	wavelength m
ν	=	wave number cm^{-1}
τ_ν	=	optical depth
j_ν	=	emissivity at wavenumber
α	=	absorption coefficient cm^{-1}
B_ν	=	Planck function

Subscripts

$H2O$	=	water vapor
$CO2$	=	carbon dioxide
cc	=	combustion chamber
w	=	wall
g	=	free stream gas
c	=	coolant
sat	=	saturation

v = at wave number

II. Introduction

Tartarus is a student-led liquid rocketry project at the University of Alabama in Huntsville as a part of the University's Space Hardware Club. The team is currently in the fabrication and testing phase of development, having completed the manufacturing of the Prometheus engine and moving into preliminary waterflow testing. During the analysis phase of this project, Grissom [1] and Shine's [2] methods were utilized to determine the film cooled length of Prometheus. These methods utilize either approximations or averages across the entire chamber to find a film cooled length. These methods are adequate in many cases and reduce computational complexity compared to a more precise method, but they also introduce uncertainty and error into their models, which makes the prediction of their engine's performance significantly more difficult. Comparatively, a line-by-line approach computes the radiated heat to a high precision utilizing the radiative heat transfer equation in a CFD or Q1D model. Due to the high computation costs of the line-by-line method in a CFD model, it is primarily used as a benchmark to validate simplified models rather than to directly analyze an engine's performance. However, a Q1D model can simplify this computation while also remaining at a high enough resolution to give informative results. In this paper, the team outlines the required steps to develop and the results of this Q1D approach.

III. Previous Methods

Due to the team still being in the midst of the hotfire campaign and therefore having no test data for Prometheus, to validate the line-by-line model, two well-accepted models were implemented and compared against. The first of these methods, and the method that Prometheus was originally analyzed with, was developed by Dr. William Grissom. Grissom's [1] model utilizes empirical approximations to determine the expected radiative heat transfer and transpiration correlated convective heat transfer coefficient as functions of the distance from the head end of the engine. This is then coupled with an empirical correlation for convective heat transfer to find the total heat flux at an arbitrary point along an engine contour. In Grissom [1], the emissivity is defined by Eq. (1).

$$\varepsilon_f = K_{pf}\varepsilon_f\left(1 + \left(\frac{\rho_{opt}}{c}\right)^{-n}\right)^{-1/n} \tag{1}$$

The values of ε_f and K_{pf} are specific to each species. Emissivity for water vapor and carbon dioxide is defined as follows.

$$K_{p(H2O)} = 1 + c_1\left(1 - exp\left[\frac{1+N_{H20}}{c_2}\right]\right) \tag{2}$$

$$c_1 = 0.26 + 0.74exp(-0.25\rho_{H2O}) \tag{3}$$

$$c_2 = 0.75 + 0.31exp(-10\rho_{H2O}) \tag{4}$$

$$\varepsilon_{f(H2O)} = 0.825 \tag{5}$$

$$K_{p(CO2)} = 0.036\rho_{CO2}^{-0.489}\left[1 + (2log(p_{cc}))^{-m}\right]^{-1/m} \tag{6}$$

$$m = 100\rho_{CO2} \tag{7}$$

$$\varepsilon_{f(CO2)} = 0.231 \tag{8}$$

The values of c and n in Eq. 1 are determined from Table 1 by performing a quadratic interpolation across temperature values. This data is drawn from Grissom [1].

Table 1: Empirical Correlation of Gas Properties

	T(K)	c(atm*m)	n
H_2O	1000	0.165	0.45
	2000	0.90	0.65
	3000	2.05	0.61
CO_2	1000	0.05	0.6
	2000	0.075	0.6
	3000	0.15	0.6

The optical densities are defined by the following equations:

$$\rho_{H2O} = Lp_{H2O} \tag{9}$$

$$\rho_{CO2} = Lp_{CO2} \tag{10}$$

$$\rho_{opt} = \rho_{H2O} + \rho_{CO2} \tag{11}$$

The emissivity is computed for both upstream and downstream effective length; these emissivity values are then averaged. The equations for both effective lengths are defined in Eq. (12) and (13).

$$L_1 = A_w^{-0.85}(0.95D_x) \tag{12}$$

$$L_2 = A_w^{-0.85}(0.95D_{cc}[\frac{4x}{D+4x}]) \tag{13}$$

Then, to compute the final total emissivity, a correction term is required to account for overlapping emissivity bands of water vapor and carbon dioxide. This term is defined in Eq. (14).

$$\Delta\varepsilon = 0.0551K_x[1 + exp(-4\rho_{opt})][1 - exp(-12.5\rho_{opt})] \tag{14}$$

$$K_x = 1 - |\frac{2N_{H2O}}{N_{H2O}+N_{CO2}}|^{n_{Kx}} \tag{15}$$

$$n_{Kx} = 5.5[1 + (1.09\rho_{opt})^{-3.88}]^{-1/3.88} \tag{16}$$

$$\varepsilon_T = \varepsilon_{H2O} + \varepsilon_{CO2} - \Delta\varepsilon \tag{17}$$

The convective heat transfer coefficient must also be computed; this is done as follows.

$$h_o = K_t G c_{pg} St_o \tag{18}$$

$$K_t = 1 + 4e_t \tag{19}$$

$$St_o = 0.5C_f Pr^{-0.6} \tag{20}$$

$$C_f = 0.0592Re_x^{-0.2} \tag{21}$$

$$Re_x = G(\frac{x_e}{\mu_g}) \tag{22}$$

$$x_e = 3.53D(1 + (\frac{x}{3.53D})^{-1.2})^{-1/1.2} \tag{23}$$

$$G = G_{cc}(\frac{T_g}{T_{mean}})(\frac{(u_g - u_c)}{u_g}) \tag{24}$$

$$G_{cc} = \rho_g u_g \tag{25}$$

$$T_{mean} = 0.5(T_g + T_{sat}) \tag{26}$$

The film cooled length is heavily dependent on the velocity of the liquid coolant. Grissom [1] determines this value implicitly through Couette flow relations as follows.

$$\Gamma_c = \frac{\dot{m}_c}{D\pi} \tag{27}$$

$$u_c = \frac{\Gamma_c}{\rho_c t} \tag{28}$$

$$t = \sqrt{\frac{2\mu_c \Gamma}{\rho_c \tau_w}} \tag{29}$$

$$\tau_w = 0.5C_f G(u_g - u_c) \tag{30}$$

The convective heat transfer then must be calculated. This value is reliant on the local heat transfer coefficient calculated above. However, the transpiration effects are in turn reliant on the convective heat transfer coefficient, and therefore these values must be computed implicitly. This is done as shown below. Note that $a = 0.6\ if\ M_v < M_g$, and $a = 0.35\ if\ M_v > M_g$.

$$h = \frac{h_o ln(1+H)}{H} \tag{31}$$

$$H = \frac{c_{pg} K_M \dot{m}_v}{h} \tag{32}$$

$$K_M = (\frac{M_g}{M_v})^a \tag{33}$$

$$\dot{m}_v = \frac{h\Delta T + \sigma A_w \varepsilon_T (T_g^{\ 4} - T_{sat}^{\ 4})}{H_{vap}} \tag{34}$$

The mass flow rate of coolant per circumferential distance, Γ_c is calculated at a set spacing down the length of the chamber.

The temperature of the liquid is defined by Eq. (35) while the temperature is less than the saturation temperature. Then, once the temperature has reached the saturation temperature, $\frac{d\Gamma_c}{dx}$ is computed following Eq. (36) until $\Gamma_c = 0$. The final value of x is then defined as the film cooled length.

$$\frac{dT}{dx} = \frac{\dot{m}_v H_{vap}}{\Gamma_c c_p} \quad (35)$$

$$\frac{d\Gamma_c}{dx} = \frac{\dot{m}_v dx}{u_c} \quad (36)$$

The second method was developed by Shine [2]. Shine's [2] method is also reliant on Leckner's [3] emissivity correlations to determine the total emissivity of water vapor and carbon dioxide. Leckner's work determined a model that defines emissivity as a function of optical path length, total pressure of the gas, and the temperature of the gas. Additionally, Leckner [3] introduced an equivalent pressure term to simplify the necessary pressure corrections. This model is represented by Eqs. (37-41). In Eq. (39), c_{ji} are a series of constants that can be found in Ref. [3]. The following application of Leckner's [3] equations comes from Ref. [4].

$$\varepsilon(p_a L, p_a, T_g) = \varepsilon_0(p_a L, T)(\frac{\varepsilon}{\varepsilon_0})(p_a L, p_a, T_g) \quad (37)$$

$$(\frac{\varepsilon}{\varepsilon_0})(p_a L, p, T_g) = [1 - \frac{(a-1)(1-P_E)}{a+b-1+P_E} exp(- c[log\frac{(p_a L)_m}{p_a L}]^2)] \quad (38)$$

$$\varepsilon_0(p_a L, T_g) = exp(\sum_{i=0}^{M}\sum_{j=0}^{N} c_{ji}(\frac{T_g}{T_0})^j(log\frac{p_a L}{(p_a L)_0})^i) \quad (39)$$

$$P_{EH2O} = P(1 + 4.9\frac{p_a}{P}\sqrt{\frac{273}{T}}) \quad (40)$$

$$P_{ECO2} = P(1 + 0.28\frac{p_a}{P}) \quad (41)$$

Then total emissivity can be calculated with Eq. (42) and Eq. (43), noting that the emissivity of water vapor and carbon dioxide should be calculated at their respective partial pressures, and that $\Delta\varepsilon$ is a correction factor representing any overlap in the emissivity bands of water vapor and carbon dioxide.

$$\varepsilon_T = \varepsilon_{H2O} + \varepsilon_{CO2} - \Delta\varepsilon \quad (42)$$

$$\Delta\varepsilon = (\frac{\zeta}{10.7+101\zeta} - 0.0089\zeta^{10.4})(log\frac{(p_{H2O}+p_{CO2})L}{(p_a L)_0})^{2.76} \quad (43)$$

$$\zeta = \frac{p_{H2O}}{p_{H2O}+p_{CO2}} \quad (44)$$

The convective heat transfer coefficient from the hot gas to the coolant, h^*_{fg}, is calculated from the saturation temperature, specific heat capacity, and enthalpy of vaporization of the coolant.

$$h^*_{fg} = h_{fg}(T_{sat,c} - T_{c1})c_{cl} \quad (45)$$

Radiative heat flux is then calculated using the temperature of the chamber, emissivity, and the Stefan Boltzmann constant.

$$q_{rad} = \varepsilon_T \sigma T^4 \quad (46)$$

Using radiative heat flux and heat transfer coefficient from Eq. (45) the blowing ratio F can be calculated using the following equation.

$$F = St\frac{c_{pg}}{h^{*}_{fg}}[(T - T_{sat,c}) + \frac{q_{rad}}{h_0}] \tag{47}$$

The blowing ratio combined with the mass velocity, G, found by the product of the density and the velocity of the free stream gas, will give the coolant evaporation rate per unit area $\dot{m}_v$.

$$\dot{m}_v = FG \tag{48}$$

The coolant flow per circumference available for film cooling, Γ_c, is defined by Eq. (49). This is a simplified form as entrainment effects were found to be negligible, likely due to a relatively low chamber pressure.

$$\Gamma_c = \frac{\dot{m}_c}{\pi D} \tag{49}$$

Then, finally, film cooled length is calculated with Eq. (50).

$$L_c = \frac{\Gamma_c}{\dot{m}_v} \tag{50}$$

IV. Line-by-Line Radiation Model

The line-by-line model differs from Grissom [1] and Shine [2] by taking the chamber to be a discrete field and solving the complete radiative heat transfer equation. Doing so yields a function of the path and the emissivity coefficient along this path, and results in the energy reflected in the direction of this path.

$$I(n, s_1) = \int_0^{\infty} I(n, s_1, \lambda)d\lambda \tag{51}$$

$$I_\nu(n, s_1) = I_\nu(n, s_0)e^{-\tau_\nu(s_0, s_1)} + \int_{s_0}^{s_1} (j_\nu(s)e^{-\tau_\nu(s, s_1)})ds \tag{52}$$

The first term of Eq. (52) describes the reflected radiative energy for an arbitrary wavelength traveling on a particular path through the engine. However, this term is reliant on all prior times that this particular ray was reflected and therefore necessitates a recursive method. Additionally, this term is commonly evaluated to equal zero due to the optical thickness of the gas. As such, this term becomes small enough in comparison to the second term to be neglected if it is calculated for all view angles at the same arbitrary point on the chamber wall for an arbitrary angle. Therefore, Eq. (52) can be simplified to Eq. (53) with very little loss of precision.

$$I_\nu(s_1) = \int_{s_0}^{s_1} (j_\nu(s)e^{-\tau_\nu(s, s_1)})ds \tag{53}$$

This function outputs the line intensity at a specific wavenumber for a specific ray through the engine. The optical density and emissivity are both derived from the absorption coefficient using Eq. (54) and Eq. (55). Note that $B_\nu(T)$ is the Planck function at a given wavenumber and temperature. Given that our gas is assumed to be insentropic Eq. (54) dependence on thermal equilibrium is met.

$$j_\upsilon(s) = \alpha_\nu(s)B_\nu(T) \tag{54}$$

$$\tau_\upsilon(s_0, s_1) = \int_{s_0}^{s_1} \alpha_\nu(s)ds \tag{55}$$

Eqs. (51-55) are from Ref. [5]. Deriving the absorption coefficient for the gas mixture requires taking into account temperature, pressure, and gas composition. However, this functional relationship is rather difficult to derive and implement as it is heavily reliant on quantum mechanical effects and properties of different isotopologues. Due to this, the data for the absorption coefficient at every wave number was retrieved from the HITEMP [6-8] chemical property database, utilizing the HAPI [9] api in Python. Below are figures displaying the absorption coefficient by wavenumber for carbon dioxide at ambient conditions, carbon dioxide at chamber temperatures, and for the gas mixture of the combusted products at chamber conditions.

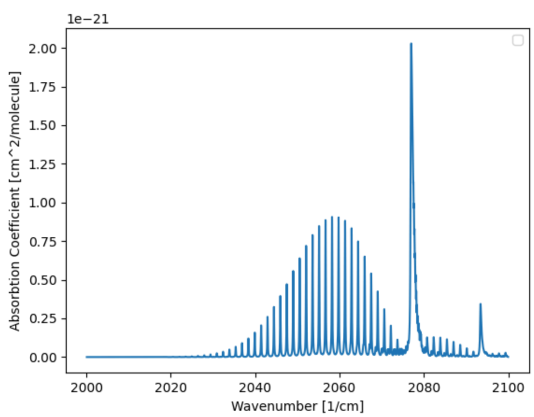

Fig. 1: Absorption Coefficients for CO_2.

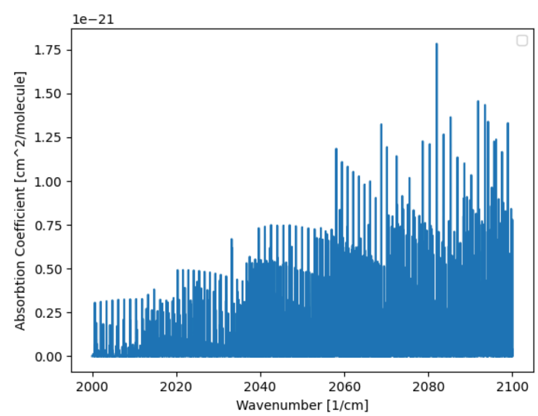

Fig. 2: Absorption Coefficients for CO_2 at Chamber Conditions.

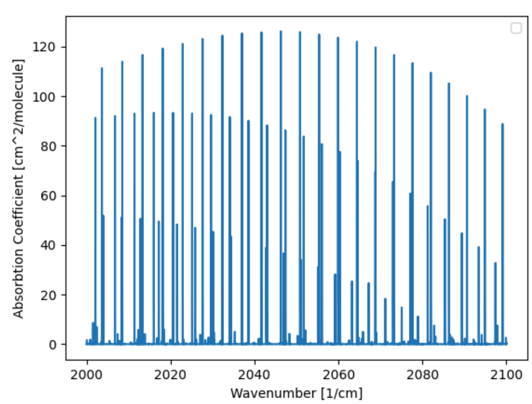

Fig. 3: Absorption Coefficients for CO_2, CO, and H_2O at chamber conditions.

Morse [10] previously developed a Q1D isentropic mode of the Prometheus engine. This model can be utilized to construct a Q1D mesh that includes the temperature, pressure, and absorption coefficient at every wavelength. This model can then be further simplified by assuming that the chamber is radially symmetric. Doing so results in a mesh that is significantly simplified from a high-fidelity CFD model. Utilizing a raytracing algorithm through this mesh then allows for the discrete numerical integration of Eq. (53), the output of which is a radiant line intensity.

V. Film Cooled Length

The radiant heat flux values calculated in the previous section can then be integrated using Eq. (56) from Refs [5]. Note that line intensity is not strictly a function of theta; instead, the two values of theta are used to determine the pointing vector V.

$$\dot{Q}_{rad} = \int_{-\pi}^{\pi}\int_{-\pi}^{\pi} I(\theta_1, \theta_2)\frac{V\bullet n}{|V||n|}d\theta_1 d\theta_2 \tag{56}$$

The calculated radiative heat transfer values can then be utilized to determine the film cooled length. This is done following a slightly modified version of the methods outlined by Shine [2] and summarized in section two. Shine's methods [2] are followed as opposed to Grissom's [1], as they claim to have compared several potential methods before settling on the method providing the best results. Shine's method [2] for calculating constant convective heat transfer without transpiration and the methodology for average coolant velocity are utilized. Additionally, the required skin friction coefficients are determined from Grissom's method [1]. Shine's method [2] is not intended for use with a nonuniform radiation value, so the length down the chamber of the engine that provides the required surface area to evaporate all of the liquid coolant is determined using Eq. (57). Note that this function must be implicitly solved for the film cooled length x.

$$\dot{m}_c H_{vap} = x(D)(\frac{1}{x}\int_0^x \dot{Q}_{rad}(x)dx + \dot{Q}_{conv}) \tag{57}$$

VI. Results

Each of the three methods outlined were used to analyze the Prometheus engine. For the line-by-line model, the input values listed in Table 2 were used. Out of the 250 cells generated, the radiative heat transfer values were only calculated for 155. These cells correlated to 3.566 inches down the chamber, which is well within the converging section of the nozzle. More specific details about the Prometheus engine can be obtained from [10]. The radiative heat transfer calculated using the line-by-line model is plotted against the distance from the injector in Fig. 4. The final film cooled length calculated by each method is displayed in Table 3.

Table 2: Resolution Parameters

Mesh Resolution	θ_1 Resolution	θ_2 Resolution
250	35	35

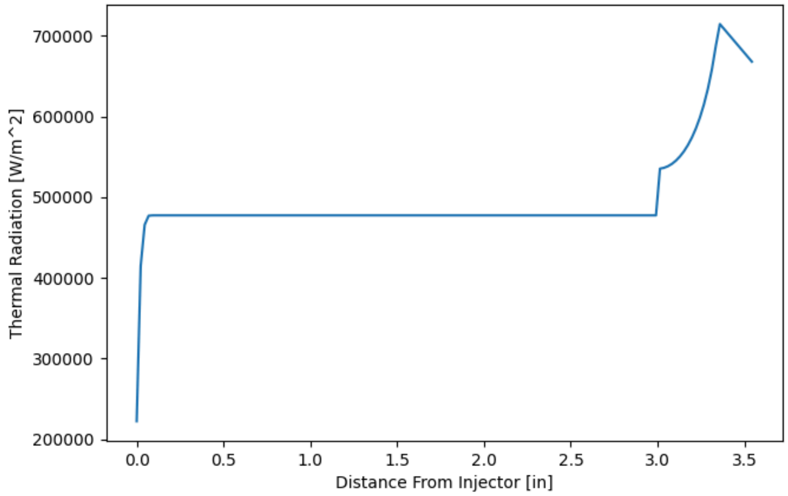

Fig. 4: Calculated Thermal Radiation

Table 3: Calculated Film Cooled Length [in]

Grissom	Shine	Line-by-Line
2.1	2.9	2.6

VII. Conclusion

While the computed values are very promising, the team will be applying all of the outlined methods to an engine that has published experimental results. This will allow for a direct side-by-side comparison of each model and allow for the final validation steps for the line-by-line method. Additionally, the team hopes to apply this work to a number of new tools to further refine the analysis of film cooled rocket engines. The first of which is a model of the convective heat transfer from the film coolant into the wall of the chamber. This project can then be utilized to develop an in-house thermal finite element analysis model that would couple the analysis of the cooling capacity of the film coolant with the temperature at a point on the wall of a chamber. Such a model would be able to capture the heat transfer within the chamber walls while directly updating the cooling capacity of the film.

Acknowledgements

The authors would first and foremost like to thank Dr. Gang Wang and Dr. Richard Tantaris for their mentorship to The University of Alabama in Huntsville's Space Hardware Club. We would also like to thank Mr. Lorenzo Coley for representing AIAA at The University of Alabama in Huntsville. We are also very grateful to the MAE department at UAH and Mr. Jon Buckley in particular for the use of their machine shop, and mentoring in manufacturing techniques. The Alabama Space Grant Consortium and the University of Alabama in Huntsville have graciously given us the resources necessary to fund this project through the Space Hardware Club. Thank you especially to AVCO for giving insightful technical feedback and providing cryogenic valves for the Modular Fluids System. Thank you to Swagelok for their generous donation and as well to MiTiGen for their in-kind contribution and support. Finally, we would like to thank all members of Tartarus for their continued support and dedication to the project.

References

[1] Grissom, W. M., "Liquid Film Cooling in Rocket Engines," Tech. Rep. AEDC-TR-91-1, Air Force Arnold Engineering Development Center (AEDC), Mar. 1991.

[2] Shine, S. R., Sunil Kumar, S., and Suresh, B. N., "A New Generalised Model for Liquid Film Cooling in Rocket Combustion Chambers," International Journal of Heat and Mass Transfer, Vol. 55, No. 19-20, 2012, pp. 5065–5075.

[3] Leckner, B., "Spectral and Total Emissivity of Water Vapor and Carbon Dioxide," Combustion and Flame, Vol. 19, No. 1, 1972, pp. 33–48.

[4] Kreith, F., and Others, The CRC Handbook of Mechanical Engineering, CRC Press, 2004.

[5] Modest, Michael, F., *Radiative Heat Transfer,* 3rd ed., Elsevier Inc., Amsterdam, 2013.

[6] Rothman, L., Gordon, I., Barber, R., Dothe, H., Gamache, R., Goldman, A., Perevalov, V., Tashkun, S., and Tennyson, J., "HITEMP, the high-temperature molecular spectroscopic database," Journal of Quantitative Spectroscopy and Radiative Transfer, Vol. 111, No. 15, 2010, pp. 2139–2150. https://doi.org/https://doi.org/10.1016/j.jqsrt.2010.05.001, URL https://www.sciencedirect.com/science/article/pii/S002240731000169X, xVIth Symposium on High Resolution Molecular Spectroscopy (HighRus-2009).
[7] Hargreaves, R. J., Gordon, I. E., Huang, X., Toon, G. C., and Rothman, L. S., "Updating the carbon dioxide line list in HITEMP," Journal of Quantitative Spectroscopy and Radiative Transfer, Vol. 333, 2025, pp. 109–324. https://doi.org/https://doi.org/10.1016/j.jqsrt.2024.109324, URL https://www.sciencedirect.com/science/article/pii/S002240732400431X.
[8] Li, G., Gordon, I. E., Rothman, L. S., Tan, Y., Hu, S.-M., Kassi, S., Campargue, A., and Medvedev, E. S., "Rovibrational Line Lists for Nine Isotopologues of the CO Molecule in the X1Σ+ Ground Electronic State," The Astrophysical Journal Supplement Series, Vol. 216, 2015, p. 15. https://doi.org/10.1088/0067-0049/216/1/15.
[9] Kochanov, R., Gordon, I., Rothman, L., Wcisło, P., Hill, C., and Wilzewski, J., "HITRAN Application Programming Interface (HAPI): A comprehensive approach to working with spectroscopic data," Journal of Quantitative Spectroscopy and Radiative Transfer, Vol. 177, 2016, pp. 15–30. https://doi.org/https://doi.org/10.1016/j.jqsrt.2016.03.005, URL https://www.sciencedirect.com/science/article/pii/S0022407315302466, xVIIIth Symposium on High Resolution Molecular Spectroscopy (HighRus-2015), Tomsk, Russia.
[10] Morse, A., Moore, Z., Cartwright, C., Jones, S., Masters, P., and Williams, J., "The Preliminary Structural and Thermal Modeling of a Small Student-Developed Liquid Rocket Engine," AIAA Paper 2024-86250, 2024.
[11] Dullemond, C. P., "Radiative Transfer in Astrophysics: Theory, Numerical Methods and Applications," , n.d. URL https://www.ita.uni-heidelberg.de/~dullemond/lectures/radtrans_2012.